PHYSICAL REVIEW A VOLUME 45, NUMBER 5 1 MARCH 1992

Electron-impact excitation of the *T* and *V* states of ethylene: An *ab initio* study

T. N. Rescigno
Lawrence Livermore National Laboratory, P.O. Box 808, L-438, Livermore, California 94550

B. I. Schneider*
Theoretical Division, T-12, Los Alamos National Laboratory, Los Alamos, New Mexico 87545

(Received 1 October 1991)

We report total and differential cross sections for electron-impact excitation of the T ($\tilde{a}\,{}^3B_{1u}$) and V (${}^1B_{1u}$) states of ethylene from threshold to 20 eV. The calculations were carried out using the complex Kohn variational method. For collision energies above the threshold for excitation of the V state, we carried out three-state close-coupling calculations using accurate multiconfiguration target states. An averaged natural orbital technique was used to obtain a compact representation of the V-state wave function that properly reflects the mixed valence-Rydberg character of this state. The total and small-angle differential cross sections for exciting the optically allowed V state are sensitive to the inclusion of high partial-wave contributions, which were computed using a simple perturbative scheme. In the energy range between the T and V states, where only two electronic states are open, we carried out dressed two-state calculations using optical potential techniques to incorporate the effect of closed channels. We found significant d-wave resonance behavior in the T-state excitation cross section near 5 eV. At higher energies, the T-state differential cross sections are backward peaked, while the V state cross sections show strong forward peaking that is typical of an optically allowed transition.

PACS number(s): 34.80.Gs

I. INTRODUCTION

For many years theoretical treatments of the electron scattering from complex polyatomic molecules were limited to electronically elastic scattering, often using model potentials and excluding electron exchange. Reliable computational methods for treating electronic excitation were absent. In addition, the difficulties of performing the necessary differential and integral cross-section measurements were such that accurate data for many molecules simply did not exist. Since these data are needed for many practical applications, including plasma chemical processing and deposition, gas laser modeling, astrophysical processes and atmospheric modeling, as well as for fundamental spectroscopic purposes, the need for reliable theoretical methods is especially acute. To exacerbate matters even further, these cross sections are often required for transient species such as free radicals or molecular fragments which are difficult to prepare and/or detect in the laboratory.

We have developed and successfully applied the complex Kohn variational method (CKVM) [1,2] to both diatomic [3–7] and polyatomic [8–11] electron-molecule scattering problems. The CKVM has proven to be a reliable tool for the study of the elastic and electronically inelastic scattering of electrons from polyatomic molecules. Our approach is *ab initio* in the sense that we solve the Schrödinger equation from first principles without the introduction of any arbitrary parameters or experimental information. Both the target wave function of the molecule and the scattering wave function at short range are determined variationally using a linear combination of Gaussian orbitals to describe the electrons. To account for the asymptotic regions in the scattering channels, the Gaussian basis set is augmented by a set of "free" functions for each open channel. The Kohn variational principle [12] for the T matrix is used to determine the optimal coefficients in the expansion. Since one of these coefficients is associated with the outgoing scattered wave, it is possible to extract a variationally stable T matrix from the solution of a set of algebraic equations whose dimensionality is determined by the number of open channels retained in the calculation.

In contrast to a number of other approaches, the CKVM is based on a Hamiltonian formulation of the scattering problem. This feature makes it possible for us to take advantage of many of the tools of modern electronic-structure theory in calculating most of the required matrix elements. In our formulation of the Kohn method, which makes use of separable expansions to eliminate large classes of continuum matrix elements [13], the only additional matrix elements required are a relatively small set of free-free and bound-free integrals. These are efficiently computed using three-dimensional numerical quadrature [14]. A detailed account of the procedure can be found in our earlier publications [5,7,10,14–16]. The electronic-structure codes we employ [17] allow us to use correlated target states as well as optical potentials derived from large scale configuration-interaction (CI) calculations to include final-state correlations. In essence the scattering calculation may be viewed as an elaborate electronic-structure calculation on the wave function of the transient negative ion which is connected to the outside world by the free-free and bound-free integrals needed to correctly describe the asymptotics.

In this paper we report results for the $(\pi \rightarrow \pi^*)$ electron-impact excitation of ethylene (C_2H_4). Ethylene is important as an industrial gas and as a prototype for heavier hydrocarbons; it has been studied experimentally by a number of researchers. These experiments have provided useful information on the total and momentum-transfer cross section for low-energy electron collisions with C_2H_4. However, little information currently exists on angularly resolved elastic or state-specific electronically inelastic scattering of electrons by C_2H_4.

The low-energy elastic scattering of electrons by C_2H_4 contains two prominent features: a Ramsauer-Townsend (RT) minimum at ~200 meV [18,19] and a shape resonance of $^2B_{2g}$ symmetry at 1.8 eV [20]. The resonance is of the π^* type, quite similar to the well-known shape resonance in N_2 [21]. The width of the resonance is larger than that in N_2 and vibrationally resolved measurements [22] reveal a much less detailed structure consistent with a shorter-lived negative ion. Recent complex Kohn variational calculations [11] on the elastic scattering of electrons from C_2H_4 using optical potentials constructed from large-scale CI calculations have confirmed the existence of the RT minimum at 200–300 meV in C_2H_4 and have produced a B_{2g} shape resonance at 1.84 eV with a width of 460 meV, in excellent agreement with available experimental information [20]. The calculation was notable in that it was the first to confirm the existence of a RT minimum in a molecule possessing a permanent quadrupole moment and suggests that such minima may exist in the cross sections for many nonpolar molecules.

The experimental situation for electronically inelastic scattering in C_2H_4 is far less satisfactory. There have been several electron-energy-loss measurements that identify the positions of a few of the excited states of the molecule [23,24], a few trapped-electron experiments [25,26] that report threshold excitation functions for a few transitions, and some relative differential cross-section experiments [27] that show the qualitative features expected of forbidden versus allowed transitions in any atomic or molecular target. We reserve further discussion of these experiments for Sec. IV of the present paper.

II. THEORY

The complex Kohn method has been described in previous papers in some detail. We will only give a brief summary here and concentrate on those aspects of the formulation most relevant to the problem at hand, namely, the generation and use of accurate multiconfiguration target states and the special techniques needed to treat optically allowed transitions. The scattering of an electron by an N-electron target molecule in the fixed-nuclei approximation may be described by a wave function of the form

$$\begin{aligned}\Psi_{\Gamma_0}(\mathbf{r}_1,\mathbf{r}_2,\ldots,\mathbf{r}_{N+1}) &= \sum_{\Gamma} \mathcal{A}[\chi_\Gamma(\mathbf{r}_1,\mathbf{r}_2,\ldots,\mathbf{r}_N)F_{\Gamma\Gamma_0}(\mathbf{r}_{N+1})] \\ &\quad + \sum_{\mu} d_\mu^{\Gamma_0}\Theta_\mu(\mathbf{r}_1,\mathbf{r}_2,\ldots,\mathbf{r}_{N+1}) , \end{aligned} \qquad (1)$$

where χ_Γ is an N-electron bound-state wave function of the target, $F_{\Gamma\Gamma_0}$ the scattering wave function for an electron incident in channel Γ_0, and Θ_μ a set of square-integrable $(N+1)$-electron wave functions used to describe "penetration," polarization, and electron correlation effects not present in the open channel (first sum) portion of Eq. (1). The antisymmetrizer $\mathcal{A}$ ensures that the overall wave function changes sign when any two electronic coordinates are interchanged.

In the complex Kohn method the scattering functions $F_{\Gamma\Gamma_0}$ are themselves expanded as a linear combination of bound functions, as well as outgoing continuum functions, g_l^Γ and regular continuum functions f_l^Γ, which behave asymptotically as

$$\begin{aligned} f_l^\Gamma(r) &\underset{r\rightarrow\infty}{\sim} \frac{\sin(k_\Gamma r - l\pi/2)}{\sqrt{k_\Gamma}} , \\ g_l^\Gamma(r) &\underset{r\rightarrow\infty}{\sim} \frac{\exp[i(k_\Gamma r - l\pi/2)]}{\sqrt{k_\Gamma}} , \end{aligned} \qquad (2)$$

where k_Γ is a channel momentum. Rather than the "conventional" choice for the outgoing continuum basis functions, which is simply to use Ricatti-Hankel functions regularized at the origin with an arbitrary cutoff function, we use the dynamically determined functions [16,28]

$$g_l^\Gamma(r) = \mathcal{G}_l^+ V \Big/ \int V F_l , \qquad (3)$$

where $\mathcal{G}_l^+$ is the partial-wave free-particle Green's function, V is any short-range function (we use a simple exponential), and F_l is the regular Ricatti-Bessel function. It is simple to show that this function satisfies the asymptotic form specified in Eq. (2). We found that this choice for the continuum basis functions gave much better convergence than the conventional one.

In practical applications both χ_Γ and Θ_μ are expanded as linear combinations of configuration state functions (CSF's) which are themselves constructed from antisymmetrized products of one electron orbitals. The $F_{\Gamma\Gamma_0}$ are required to be orthogonal to the entire set of orbitals used in the construction of the CSF's in order that the overall $(N+1)$-electron functions form an orthonormal set. Therefore a subset of the Θ_μ, the so-called penetration terms [29,30], are introduced in order to compensate for the orthogonality constraint imposed between the $F_{\Gamma\Gamma_0}$ and the molecular orbitals used to construct the target wave functions. A more detailed discussion of Eq. (1) can be found in Ref. [5]. For the purpose of this discussion it is important to note that, since the size of the scattering space depends on the product of the number of target CSF's times the number of scattering functions, it is desirable to keep the orbital set used in the construction of the target CSF's as small as possible. Moreover, if we can achieve a compact representation of the target states in terms of a small set of molecular orbitals, then the number of penetration terms needed to relax orthogonality constraints can also be made small. We have recently shown [5] that close-coupling calculations which employ a large number of variationally determined penetration terms can be plagued by pseudoresonances at intermediate energies unless these terms are appropriately restricted. Thus it is essential to invoke methodologies which reduce the molecular-orbital subspace used to construct the target CSF's to a small number. Our approach is to start with a reasonably large orbital basis, construct a configuration-interaction expansion that reproduces the major correlation effects present in the ground and excited states of the target, and to then use natural orbital techniques to drastically reduce the orbital space needed to reproduce the original CI energies and wave functions.

One of the excited states included in the present study is optically allowed from the ground state. For such dipole-allowed transitions, many partial-wave components are needed to properly describe scattering for small deflection angles of the incident electron and to obtain converged total cross sections. The reason is that the underlying direct transition potential for such transitions gives rise to a long-range interaction which behaves asymptotically as $\mathbf{D}\cdot\mathbf{r}/r^3$, where $\mathbf{D}$ is the transition dipole moment.

It is neither possible nor necessary to carry the full complement of partial waves in a coupled-channel variational calculation to obtain converged cross sections. Beyond a certain l cutoff, the partial-wave components of the scattering functions do not penetrate the interior part of the molecular target. In this weak-scattering limit, it is sufficient to employ a perturbative treatment such as the Born approximation. There is a considerable literature on the subject of electronically elastic scattering of electrons by polar molecules [31], where similar considerations about the underlying electron dipole interaction apply. In many of these studies, a Born closure formula is used to accelerate convergence of integral and differential cross sections. The same general considerations apply to the case of excitation cross sections for optically allowed transitions. However, the way we implement Born closure differs from the procedures that are traditionally applied in several key respects. We use a numerical procedure to construct the laboratory-frame cross sections from the partial-wave T-matrix elements, rather than the analytic procedures that are typically used. This in turn allows us to apply Born closure directly to the scattering amplitudes rather than to the differential cross sections. We will describe the method in some detail below.

The partial-wave Born approximation for a particular T-matrix element contributing to an inelastic dipole-allowed process $\Gamma \rightarrow \Gamma'$ is given by

$$
{}^{B}T^{\Gamma\Gamma'}_{lml'm'} = 2\sqrt{k_\Gamma k_{\Gamma'}} \int j_l(k_{\Gamma'} r) Y^{*}_{l'm'}(\hat{\mathbf{r}})(\chi_\Gamma H \chi_{\Gamma'}) \times j_l(k_\Gamma r) Y_{lm}(\hat{\mathbf{r}}) d^3 r \; . \tag{4}
$$

Consistent with this approximation is the replacement of the transition potential by its asymptotic form [32]

$$
\begin{aligned}
V_{\Gamma\Gamma'}(\mathbf{r}) &= (\chi_\Gamma H \chi_{\Gamma'}) \\
&\equiv \int \chi_\Gamma(\mathbf{r}_1, \ldots, \mathbf{r}_N) H(\mathbf{r}, \mathbf{r}_1, \ldots, \mathbf{r}_N) \chi_{\Gamma'}(\mathbf{r}_1, \ldots, \mathbf{r}_N) \\
&\sim \mathbf{D}\cdot\hat{\mathbf{r}}/r^2 \; ,
\end{aligned} \tag{5}
$$

where $\mathbf{D}$ is the transition dipole moment for the transition in question and $\hat{\mathbf{r}}$ is a unit vector in the body frame of the molecule. In this limit, the partial-wave T-matrix elements can be evaluated in closed form [33]. It is also possible to evaluate the full-body-frame, fixed-nuclei T matrix (scattering amplitude) in this same limit [34]:

$$
\begin{aligned}
\left\langle k_{\Gamma'} \middle| {}^{B}T^{\Gamma\Gamma'} \middle| k_\Gamma \right\rangle &= -\frac{\sqrt{k_\Gamma k_\Gamma{}'}}{8\pi^2} \int e^{-i(\mathbf{k}_\Gamma - \mathbf{k}_{\Gamma'})\cdot\mathbf{r}} \frac{\mathbf{D}\cdot\hat{\mathbf{r}}}{r^2} d^3 r \\
&= -\frac{\sqrt{k_\Gamma k_{\Gamma'}}\, i\mathbf{D}\cdot\hat{\mathbf{k}}'}{2\pi|\mathbf{k}_\Gamma - \mathbf{k}_{\Gamma'}|} \; ,
\end{aligned} \tag{6}
$$

where $\hat{\mathbf{k}}' \equiv (\mathbf{k}_{\Gamma'} - \mathbf{k}_\Gamma)/|\mathbf{k}_{\Gamma'} - \mathbf{k}_\Gamma|$. We next write the partial-wave expansion of the exact body frame T matrix in the following form:

$$
\begin{aligned}
\langle \mathbf{k}_\Gamma | T^{\Gamma\Gamma'} | \mathbf{k}_{\Gamma'} \rangle = &-\sqrt{k_\Gamma k_{\Gamma'}}\, i\mathbf{D}\cdot\frac{\hat{\mathbf{k}}'}{2\pi|\mathbf{k}_\Gamma - \mathbf{k}_{\Gamma'}|} \\
&+ \sum_{\substack{l',l \\ m,m'}} i^{l-l'} Y^{*}_{l'm'}(\hat{\mathbf{k}}_{\Gamma'}) Y_{lm}(\hat{\mathbf{k}}_\Gamma) \\
&\times \left(T^{\Gamma\Gamma'}_{lml'm'} - {}^{B}T^{\Gamma\Gamma'}_{lml'm'} \right) \; ,
\end{aligned} \tag{7}
$$

where we have merely added and subtracted the Born approximation to the partial-wave expansion of the exact T matrix. The point to note is that the sum now contains differences between exact and Born partial-wave elements, which rapidly approach zero as l (l') get large. For C_2H_4 we found that retaining terms up to and including l (l')$=5$ was sufficient to converge the T matrix to a few percent. Note that it is essential to employ a consistent phase convention in evaluating the various contributions to Eq. (7). It is also necessary to define the transition moment $\mathbf{D}$ used in the Born approximation to the T matrix in the same coordinate system that is used in the electronic-structure calculation.

In order to obtain differential (and total) cross sections corresponding to a random orientation of the target molecule with respect to an incident electron beam in the laboratory frame, cross sections obtained from the body-frame scattering amplitude must be averaged over all orientations of the target in a laboratory-fixed coordinate frame [35]

$$
\frac{d\sigma^{\Gamma\Gamma'}}{d\Omega} = \frac{(4\pi)^2}{k_\Gamma^2} \int \frac{d\alpha\, d\cos\beta\, d\gamma}{8\pi^2} |\langle \mathbf{k}_{\Gamma'} | T^{\Gamma\Gamma'} | \mathbf{k}_\Gamma \rangle|^2 \; . \tag{8}
$$

The integration in Eq. (8) is over the three Euler angles that orient the vectors $\mathbf{k}_\Gamma$ and $\mathbf{k}_{\Gamma'}$ with respect to the target. The angle between $\mathbf{k}_\Gamma$ and $\mathbf{k}_{\Gamma'}$ is the laboratory scattering angle.

It is traditional to use rotational harmonics to express the body-frame T matrix in terms of laboratory frame angles so that the orientation dependence of T and hence the averaging required in Eq. (8) can be performed analytically [35]. This is one aspect of our treatment that differs from the usual approach. We elect to perform this integration numerically, keeping the angle between $\mathbf{k}_\Gamma$ and $\mathbf{k}_{\Gamma'}$ fixed. This approach avoids the complex angular momentum algebra necessitated by an analytic formulation [36] and substantially reduces the complexity of the coding required. Moreover, it allows us to use the Born closure formula for the T matrix, Eq. (7), directly in Eq. (8). We use numerical quadrature to evaluate Eq. (8). Starting with an initial pair of wave vectors $\mathbf{k}_{\Gamma_0}$ and $\mathbf{k}'_{\Gamma_0}$ in the body frame, we can express the wave vectors needed to evaluate the integrand [Eq. (7)] for any set of Euler angles, from the expression [37]

$$\mathbf{k}_\Gamma(\alpha,\beta,\gamma)=\begin{bmatrix}\cos(\alpha)\cos(\beta)\cos(\gamma)-\sin(\alpha)\sin(\gamma) & -\cos(\alpha)\cos(\beta)\sin(\gamma)-\sin(\alpha)\cos(\gamma) & \cos(\alpha)\sin(\beta)\\ \sin(\alpha)\cos(\beta)\cos(\gamma)+\cos(\alpha)\sin(\gamma) & -\sin(\alpha)\cos(\beta)\sin(\gamma)+\cos(\alpha)\cos(\gamma) & \sin(\alpha)\sin(\beta)\\ -\sin(\beta)\cos(\gamma) & \sin(\beta)\sin(\gamma) & \cos(\beta)\end{bmatrix}\mathbf{k}_{\Gamma_0}\ . \tag{9}$$

To appreciate the manner in which our technique differs from traditional procedures, it is instructive to examine the way in which cross sections are usually evaluated. The rotationally averaged differential cross section for an arbitrary polyatomic molecule can be expressed in terms of a completion formula that takes the form of a Legendre expansion [36]:

$$\frac{d\sigma^{\Gamma\Gamma'}}{d\Omega}=\sum_{\lambda=0}^{\infty}A_\lambda P_\lambda[\cos(\theta)]\ , \tag{10}$$

where the A_λ coefficients can be expressed in the form

$$A_\lambda=\mathbf{T}^\dagger\mathbf{X}_\lambda\mathbf{T}\ . \tag{11}$$

$\mathbf{T}$ is the partial wave T matrix and $\mathbf{X}_\lambda$ is a (complicated) symmetric matrix [36] whose explicit form need not concern us here. The essential point is that for dipole-dominated transitions, the A_λ coefficients with large λ values get most of their combination from terms involving T-matrix elements with large l values, for which the Born approximation gives good values. Therefore Eq. (10) can be well approximated as

$$\frac{d\sigma^{\Gamma\Gamma'}}{d\Omega}=\frac{d\sigma^{\Gamma\Gamma'}_{\mathrm{Born}}}{d\Omega}+\sum_{\lambda=0}^{\lambda_{\max}}(A_\lambda-A_\lambda^{\mathrm{Born}})P_\lambda[\cos(\theta)]\ . \tag{12}$$

This is the way in which Born closure was originally used to accelerate convergence by Itikawa [38], for example, and by Crawford and Dalgarno [39]. Equation (12) has also been used in more recent angular frame transformation schemes [31,40,41] as well as in recent *ab initio* [42] and model potential studies [43]. A notable exception can be found in the work of Fliflet and McKoy [44], who used the momentum-transfer representation of Siegel, Dill, and Dehmer [45] to express the differential cross section in the form of an incoherent sum before applying Born closure:

$$\frac{d\sigma^{\Gamma\Gamma'}}{d\Omega}=\sum_{j_t}|B^{j_t}(\Omega)|^2\ , \tag{13}$$

where the expansion coefficients B^{j_t} have the form

$$B^{j_t}(\Omega)=\sum_{l,m,l',m'}X_{j_t}^{lml'm'}T^{\Gamma\Gamma'}_{lml'm'}Y_{lm}(\Omega)\ . \tag{14}$$

A Born-closure formula is then applied directly to Eq. (14) and the result used in Eq. (13).

We note that Eq. (8) as well as Eq. (13), express the differential cross section as the squared modulus of an amplitude and will always produce a physical result no matter how severely the partial-wave series is truncated. This is not necessarily the case with Eq. (12), which can produce negative cross sections if the angular momentum sums are not converged. This is most likely to be a problem at large scattering angles where $d\sigma^{\Gamma\Gamma'}_{\mathrm{Born}}/d\Omega$ is not necessarily a good approximation to the true cross section. Indeed, Gibson *et al.*, [42], who used Eq. (12) in their study of excitation of the optically allowed $B\,{}^1\Sigma_u$ state of H_2, reported problems with convergence at intermediate scattering angles. We found that we could obtain convergent cross sections at any scattering angle with a relatively small number of variationally obtained T-matrix elements.

It is also interesting to note that it is possible to evaluate the scattering amplitude in the Born approximation for an arbitrary polyatomic molecule analytically when the target wave functions are expanded in Cartesian Gaussian basis functions [46]. However, the resulting expressions are considerably more complicated than what is achieved in Eq. (5) by using the simple dipole approximation to the transition potential. The essential point to bear in mind is that it is only the high-order partial-wave T-matrix elements that are needed for convergence. These terms are insensitive to the short-range part of the transition potential. The exact Born and dipole Born T-matrix elements will of course differ for small values of l (l'), but these terms cancel out of Eq. (7). Therefore the dipole Born approximation achieves a considerable computational economy without any compromise in accuracy.

III. COMPUTATIONS

Ethylene is a closed-shell molecule with a ground state (N) of ${}^1A_g$ symmetry. The first excited electronic state ($\tilde{a}$ or Mulliken's T state [47]) is of ${}^3B_{1u}$ symmetry and is located 4.6 eV vertically above the ground state, while the ${}^1B_{1u}$ state (Mulliken's V state) is located experimentally at 7.65 eV. While the ($\pi\rightarrow\pi^*$) triplet state is well characterized at the Hartree-Fock level as a valence state, characterization of the V state proved to be a difficult task for theoreticians for a number of years. Extensive *ab initio* calculations have confirmed that the V state is mostly valencelike with a small Rydberg admixture [48]. (The lowest Rydberg state of ethylene is located ~7.1 eV above the N state.) It was our desire to obtain relatively simple representations of the excited states that preserved their valence character. This is especially important for the V state since previous theoretical studies have shown that Hartree-Fock calculations produce a Rydberg-like state [49] and no single-configuration wave function was able to achieve the proper valence-Rydberg balance.

All calculations were carried out at the equilibrium geometry of the ground state ($R_{\mathrm{CC}}=1.339$ Å, $R_{\mathrm{CH}}=1.086$ Å, H-C-H$=117.6°$). The basis set we employed for the target state calculations consisted of Dunning's $(9s/5p)$ carbon basis [50] contracted to $[4s/2p]$ and Dunning's $(5s)/[3s]$ basis for hydrogen [51]. We included a set of d functions for polarization on each carbon atom ($\alpha_d=0.45$), along with a full set of diffuse p and d functions ($\alpha_p=0.05$, $\alpha_d=0.085$) at the center of mass and p functions ($\alpha_p=0.2$) on the hydrogens. The ground-state self-consistent field (SCF) energy in the basis is -78.0401 a.u. We then performed a Tamm-Dancoff CI calculation which consists of all single excitations from the ground-state SCF wave function. McMurchie and Davidson [48] have noted that such a calculation does remarkably well in describing the V state compared to their more extensive CI calculations. We next obtained natural orbitals by averaging the density matrices for the ground, T, and V states. Ordered on the basis of occupation number, the first eight natural orbitals correspond to those strongly occupied in the ground state, while the ninth orbital is a valencelike $\pi^*(b_{2g})$ orbital. We also retained the next three natural orbitals which included a $\sigma^*(b_{1u})$, a Rydberg b_{2g}, and a b_{2u} orbital. To generate the target wave functions used in the scattering calculations, the all singles CI calculations were repeated using this smaller set of twelve natural orbitals. The values we obtained for the $N\rightarrow T$ and $N\rightarrow V$ excitation energies were 3.64 and 8.20 eV, respectively, compared to the values of 3.55 and 7.90 eV we obtained using the full orbital basis. The calculated value for the out-of-plane extent of the V state, as measured by $\langle\Psi|\sum_i x_i^2|\Psi\rangle$, is very sensitive to deficiencies in either the basis or the CI [48]. We obtained a value of 14.3 for this quantity, compared to McMurchie and Davidson's best value of 17.8. Finally, the value we obtained for the $N\rightarrow V$ transition moment was 1.65 a.u., compared to McMurchie and Davidson's value of 1.76.

In order to generate the square-integrable basis orbitals for the complex Kohn variational calculations, we used the entire set of natural orbitals, less the twelve target orbitals, plus additional orbitals, depending on the total symmetry being studied, constructed from the functions listed in Table I. Finally, we included partial-wave continuum basis functions up to $l=5$, $|m|=4$ in our calculations. Details about the numerical schemes used in the evaluation of bound-free and free-free matrix elements, as well as other technical aspects of the complex Kohn method, have been given elsewhere [5–16].

We carried out three-channel calculations over the energy range from 9 to 20 eV, where the N, T, and V states are all energetically open. For these calculations, the only Q-space terms [second sum on the right-hand side of Eq. (1)] included in the trial wave function were the penetration terms generated from the dominant configuration in each target state which are needed to relax the orthogonality constraints imposed on $F_{\Gamma\Gamma_0}$. These terms are generated by considering the direct product between the target natural orbitals and the three configurations $[\;]\pi^2$, $[\;]\pi\pi^*$, ${}^3B_{1u}$, and $[\;]\pi\pi^*$, ${}^1B_{1u}$ and retaining those terms consistent with the Pauli principle. We did not use any minor components of the target wave functions to generate penetration terms since inclusion of such terms can give rise to spurious behavior at higher energies unless special projection techniques are employed. This point is discussed at length in Ref. [5].

In the energy range from 4 to 8 eV where, in our calculation only the N and T states are energetically open, we performed two-state calculations and included additional correlation terms to incorporate the effect of closed channels. The Q-space terms in this case consisted of the same penetration terms referred to above along with a class of CSF's which we have previously referred to as CI relaxation terms [10]. These terms are simply the direct products of the L^2 scattering orbitals used to expand $F_{\Gamma\Gamma_0}$ and all of the states (excluding N and V) that can be formed from the CSF's used in our target CI calculation. These terms can thus describe the effects of target distortion and polarization to the extent that the limited space of natural orbitals used can represent virtual excitation of the target. These effects become increasingly important as the collision energy decreases. Indeed, we know from our earlier study of elastic scattering in C_2H_4 that the ${}^2B_{2g}$ shape resonance we found at 1.8 eV is sensitive to target distortion effects and is pushed to higher energy when these effects are not included [11].

The cross sections we report in the following section include variational contributions from ${}^2A_g$, ${}^2B_{1u}$, ${}^2B_{2g}$, ${}^2B_{2u}$, ${}^2B_{3g}$, and ${}^2B_{3u}$ symmetry. The ${}^2B_{1g}$ symmetry

TABLE I. Cartesian Gaussian functions used to supplement the target basis set.

Center	Type	Exponent(s)
Carbon	s	0.08
Carbon	p_x,p_y,p_z	1.0
Carbon	$d_{x^2},d_{y^2},d_{xz},d_{yz}$	5.0,1.5,0.15
Carbon	d_{xy}	15.0,6.0,2.4,0.96,0.38, 0.15,0.06,0.025,0.01,0.004
Center of mass	s	0.0085,0.005
Center of mass	p_x,p_y,p_z	0.017,0.0085,0.005
Center of mass	$d_{x^2},d_{y^2},d_{z^2},d_{xz},d_{yz}$	0.04,0.02,0.01

component was found to contribute negligibly to the $N \rightarrow T$ and $N \rightarrow V$ excitation cross sections, but was included in the total (elastic plus inelastic) scattering cross sections we report. Finally, the dipole Born approximation was used to converge the $N \rightarrow V$ cross sections, as discussed above.

IV. RESULTS AND DISCUSSION

The calculated integral cross section for $N \rightarrow T$ excitation is plotted in Fig. 1 as a function of incident electron energy. For comparison, we also show, in the Fig. 1 inset, the $^3B_{1u}$, $\pi \rightarrow \pi^*$ excitation function measured by Van Veen [25] using the trapped-electron technique. We have made no attempt to shift our calculated excitation energies to coincide with experiment. Therefore, to facilitate the comparison with Van Veen's data, the cross section is also shown as a function of excess electron energy. The sharp peak near 1.4 eV in the measured excitation function is clearly seen in our calculated cross section, as well as the broad maximum at higher energy. The latter feature occurs ~1.4 eV higher in our calculated cross section than it does in Van Veen's experiment. Van Veen interprets the 1.4-eV peak as a core-excited shape resonance with the configuration $\pi(\pi^*)^2$. This would give the resonance overall $^2B_{3u}$ symmetry. However, our calculations indicate that this feature is clearly associated with the $^2B_{2g}$ symmetry component. Moreover, analysis of the optical potential revealed no isolated eigenvalue in this energy range. Our conclusion is that it is actually the tail of the low-energy $^2B_{2g}$ elastic shape resonance, which has the configuration $(\pi)^2\pi^*$, that causes a peak in the $N \rightarrow T$ excitation cross section just above threshold. To test this hypothesis we recomputed the $^2B_{2g}$ contribution to the cross section, omitting the $(\pi)^2\pi^*$ configuration from the Kohn trial wave function. This calculation gave a structureless $N \rightarrow T$ excitation cross section, which supports our analysis of the $N \rightarrow T$ threshold peak.

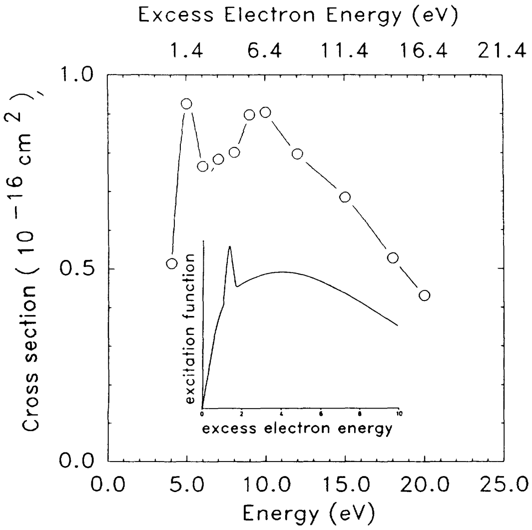

FIG. 1. Total cross section for $N \rightarrow T$ excitation in ethylene. Inset shows the $\pi \rightarrow \pi^*$ excitation function measured by Van Veen (Ref. [25]).

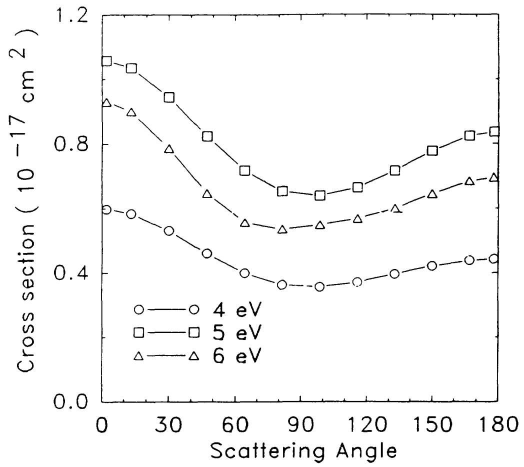

FIG. 2. Differential cross section for $N \rightarrow T$ excitation in ethylene at 4.0, 5.0, and 6.0 eV impact energy.

Further insight about the $N \rightarrow T$ excitation process can be gained by examining the differential cross sections (DCS's), which are plotted in Figs. 2–4. As Fig. 2 shows, in the vicinity of the threshold resonance peak the differential cross section has pronounced d-wave character with a broad minimum near 90°. At higher impact energies, the angular distributions become more complicated and begin to develop a pronounced backward peaking, which is typical of triplet excitation. There have been no direct measurements of the $N \rightarrow T$ differential cross section. Trajmar, Rice, and Kuppermann [27] have reported measurements of the ratio of the $N \rightarrow T$ DCS to that of the $\tilde{E}$ Rydberg state at one energy (20.4 eV above the $\tilde{a}$ state threshold) between 10° and 80°. Our results at 20 eV indicate that the $N \rightarrow T$ DCS shows only a slight increase over this angular range, in qualitative agreement with their conclusion.

Figure 5 shows our result for the $N \rightarrow V$ total cross section. To illustrate the importance of including higher partial waves, we have plotted the results obtained both

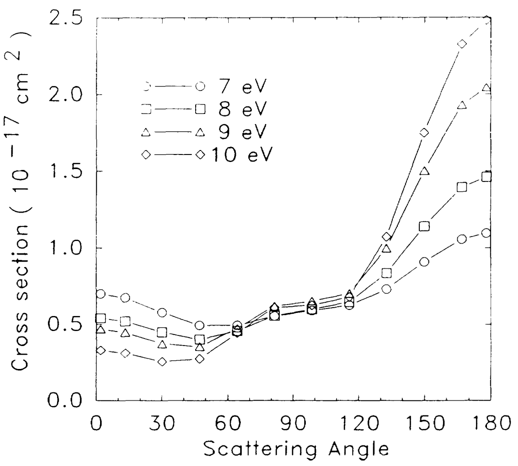

FIG. 3. Same as in Fig. 2, for 7.0, 8.0, 9.0, and 10.0 eV impact energy.

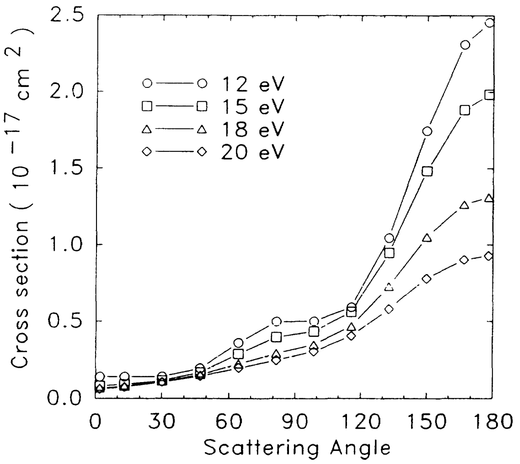

FIG. 4. Same as in Fig. 2, for 12.0, 15.0, 18.0, and 20.0 eV impact energy.

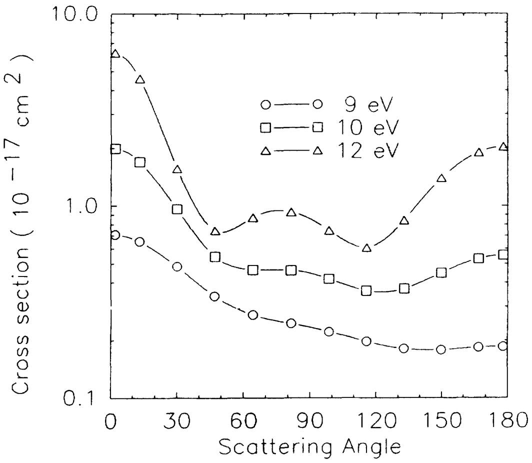

FIG. 6. Differential cross section for $N \to V$ excitation in ethylene at 9.0, 10.0, and 12.0 eV impact energy.

with and without the inclusion of the Born correction. As expected, the Born corrections become increasingly important as the energy increases. At 20 eV, the Born terms account for ~30% of the total cross section.

Figures 6 and 7 show the differential cross sections we have obtained for the $N \to V$ excitation process. Although there is some interesting structure between 30° and 120° that develops as the energy increases, the predominant characteristic we notice is that the cross sections become increasingly forward peaked as the electron-impact energy rises. This is typical of an optically allowed transition. As far as we know, there have been no direct measurements of the $N \to V$ cross section. Because of the strong overlap of the V state and the Rydberg states of ethylene, an unambiguous measurement of the $N \to V$ cross section would be quite difficult.

Sueoka and Mori [52] have measured total electron-scattering cross sections for C_2H_4 using a retarding potential time-of-flight method. To compare with their data, we have combined the elastic cross sections obtained from our CKVM calculations with the $N \to T$ and $N \to V$ excitation cross sections. The results are plotted in Fig. 8 along with the measured data of Sueoka and Mori. Several features are worth noting. The experimental data shows a minimum near 3.5 eV, approximately 1.5 eV above the ${}^2B_{2g}$ elastic shape resonance. Our cross section does show a minimum, but it occurs closer to 5 eV and is not as deep as what is found experimentally. We have already commented on the fact that the truncated set of target natural orbitals we employed in these calculations limits the extent to which low-energy target distortion can be described. As a result, the ${}^2B_{2g}$ elastic shape resonance is evidently coming out at a slightly higher energy than it should [11] and the minimum near 5 eV is consequently not deep enough. Our total cross section is also seen to be systematically lower than experiment in the energy range 7–10 eV. However, this is consistent with the fact that the total cross-section measurements include the effect of Rydberg excitations which we have not considered here. Recall that the lowest Ryd-

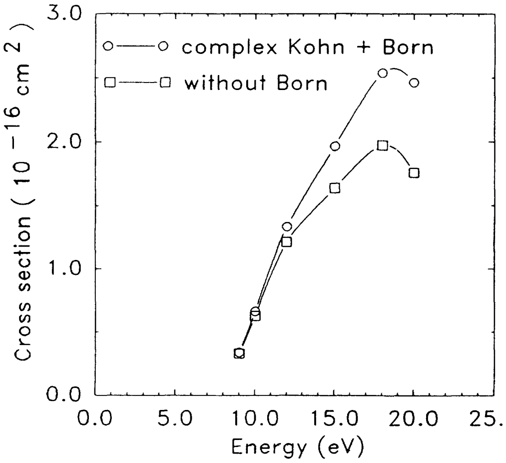

FIG. 5. Total cross section for $N \to V$ excitation in ethylene. Comparison of theoretical results obtained with and without Born correction.

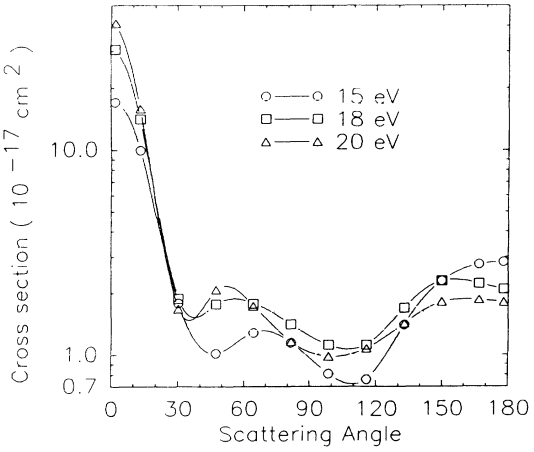

FIG. 7. Same as in Fig. 6, for 15.0, 18.0, and 20.0 eV impact energy.

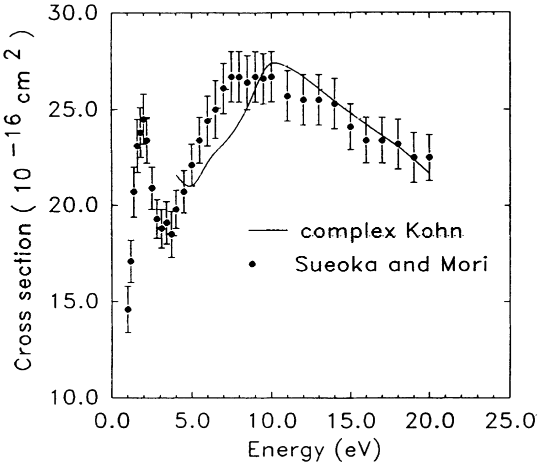

FIG. 8. Total scattering cross sections for ethylene. Comparison of theoretical results and experimental results of Sueoka and Mori (Ref. [52]).

berg state of ethylene lies 7.1 eV vertically above the ground state. Moreover, in contrast to valence-state excitation, one expects the excitation cross sections for Rydberg states to fall off rapidly from threshold. Comparison of our results with experiment therefore suggests that Rydberg excitation accounts for ~10% of the total scattering cross section in the 7–10 eV range. The sum of our elastic $N \rightarrow T$ and $N \rightarrow V$ cross sections lies within the experimental error bars from 10 to 20 eV.

V. CONCLUSIONS

We have applied the CKVM to study electron-impact excitation of the T and V states of ethylene. We have demonstrated how the CKVM allows one to carry out coupled-channel calculations of electronic excitation in a polyatomic molecule using accurate multiconfiguration target wave functions. Our intention has been to supplement the limited body of experimental data presently available on this molecule. Our calculations have confirmed the existence of resonance structure in the $N \rightarrow T$ excitation cross section near threshold and have clarified the nature of the threshold peak. Our calculations suggest that this structure arises from interaction between direct background excitation and a lower-lying $^2B_{2g}$ elastic shape resonance. We have also quantified the $N \rightarrow V$ excitation cross section, for which no direct measurements have been made. Finally, by comparing our results to measured total cross-section data, we have been able to estimate the magnitude of Rydberg excitation in this molecule.

ACKNOWLEDGMENTS

This work was performed under the auspices of the U.S. Department of Energy by the Lawrence Livermore National Laboratory and the Los Alamos National Laboratory under Contracts Nos. W-7405-ENG-48 and W-7405-ENG-36.

---

*Present address: Physics Division, National Science Foundation, Washington, DC 20550.

[1] W. H. Miller and B. M. D. D. Jansen op de Haar, J. Chem. Phys. **86**, 6213 (1987).
[2] C. W. McCurdy, T. N. Rescigno, and B. I. Schneider, Phys. Rev. A **36**, 2061 (1987).
[3] T. N. Rescigno and B. I. Schneider, J. Phys. B **21**, L691 (1988).
[4] S. D. Parker, C. W. McCurdy, T. N. Rescigno, and B. H. Lengsfield, Phys. Rev. A **43**, 3514 (1991).
[5] B. H. Lengsfield and T. N. Rescigno, Phys. Rev. A **44**, 2913 (1991).
[6] A. E. Orel, T. N. Rescigno, and B. H. Lengsfield, Phys. Rev. A **42**, 5292 (1990).
[7] A. E. Orel, T. N. Rescigno, and B. H. Lengsfield, Phys. Rev. A **44**, 4328 (1991).
[8] T. N. Rescigno, C. W. McCurdy and B. I. Schneider, Phys. Rev. Lett. **63**, 248 (1989).
[9] T. N. Rescigno, B. H. Lengsfield and C. W. McCurdy, Phys. Rev. A **41**, 2462 (1990).
[10] B. H. Lengsfield, T. N. Rescigno, and C. W. McCurdy, Phys. Rev. A **44**, 4296 (1991).
[11] B. I. Schneider, T. N. Rescigno, B. H. Lengsfield, and C. W. McCurdy, Phys. Rev. Lett. **66**, 2728 (1991).
[12] W. Kohn, Phys. Rev. **74**, 1763 (1948).
[13] T. N. Rescigno and B. I. Schneider, Phys. Rev. A **37**, 1044 (1988).
[14] C. W. McCurdy and T. N. Rescigno, Phys. Rev. A **39**, 4487 (1989).
[15] B. I. Schneider and T. N. Rescigno, Phys. Rev. A **37**, 3749 (1988).
[16] T. N. Rescigno and A. E. Orel, Phys. Rev. A **43**, 1625 (1991).
[17] P. Saxe, R. Martin, M. Page and B. Lengsfield, Lawrence Livermore National Laboratory Internal Report No. UCRL-MA-103547, 1990 (unpublished).
[18] M. J. W. Boness, I. W. Larkin, J. B. Hasted, and L. Moore, Chem. Phys. Lett. **1**, 292 (1967).
[19] M. Hayashi, in *Non-Equilibrium Processes in Partially Ionized Gases,* edited by M. Capitelli and J. N. Bardsley (Plenum, New York, 1990), p. 333.
[20] P. D. Burrow and K. D. Jordan, Chem. Phys. Lett. **36**, 594 (1975).
[21] G. Schulz, in *Principles of Laser Plasmas,* edited by G. Bekefi (Interscience, New York, 1976).
[22] I. C. Walker, A. Stamatović, and S. F. Wong, J. Chem. Phys. **69**, 5532 (1978).
[23] A. Kupperman and L. Raff, J. Chem. Phys. **37**, 2497 (1962).
[24] J. P. Doering, J. Chem. Phys. **46**, 1194 (1967).
[25] E. H. Van Veen, Chem. Phys. Lett. **41**, 540 (1976).
[26] H. H. Brongersma, A. J. H. Boerboom, and J. Kistemaker, Physica **44**, 449 (1969).
[27] S. Trajmar, J. K. Rice, and A. Kuppermann, Adv. Chem. Phys. **18**, 15 (1970).
[28] Y. Sun, D. J. Kouri, D. G. Truhlar, and D. W. Schwenke,

Phys. Rev. A **41**, 4857 (1990).

[29] H. E. Saraph, M. J. Seaton, and J. Shemming, Proc. Phys. Soc. London **89**, 27 (1966).

[30] P. G. Burke, A. Hibbert, and W. D. Robb, J. Phys. B **4**, 153 (1971).

[31] See, for example, L. A. Collins and D. W. Norcross, Phys. Rev. A **18**, 467 (1978). This paper gives a clear treatment of the subject and also contains many references to earlier work on the subject.

[32] See, for example, M. J. Seaton, Proc. Phys. Soc. London **79**, 1105 (1962).

[33] Y. Itikawa and K. Takayanagi, J. Phys. Soc. Jpn. **26**, 1254 (1969).

[34] O. H. Crawford, A. Dalgarno, and P. B. Hays, Mol. Phys. **13**, 181 (1967).

[35] See, for example, N. F. Lane, Rev. Mod. Phys. **52**, 29 (1980).

[36] See, for example, P. G. Burke, N. Chandra, and F. A. Gianturco, J. Phys. B **5**, 2212 (1972).

[37] M. E. Rose, *Elementary Theory of Angular Momentum* (Wiley, New York, 1967), pp. 62–65.

[38] Y. Itikawa, J. Phys. Soc. Jpn. **27**, 444 (1969).

[39] O. H. Crawford and A. Dalgarno, J. Phys. B **4**, 494 (1971).

[40] D. W. Norcross and N. T. Padial, Phys. Rev. A **25**, 226 (1982).

[41] J. Siegel, J. L. Dehmer, and D. Dill, Phys. Rev. A **23**, 632 (1981).

[42] T. L. Gibson, M. A. P. Lima, V. McKoy, and W. M. Huo, Phys. Rev. A **35**, 2473 (1987).

[43] F. A. Gianturco, J. Phys. B **24**, 3837 (1991).

[44] A. W. Fliflet and V. McKoy, Phys. Rev. A **21**, 1863 (1980).

[45] J. Siegel, D. Dill, and J. L. Dehmer, Phys. Rev. A **17**, 2106 (1978).

[46] K. J. Miller and M. Krauss, J. Chem. Phys. **47**, 3754 (1967).

[47] R. S. Mulliken, J. Chem. Phys. **33**, 1596 (1960).

[48] L. E. McMurchie and E. R. Davidson, J. Chem. Phys. **66**, 2959 (1977).

[49] T. H. Dunning, W. J. Hunt, and W. A. Goddard, Chem. Phys. Lett. **4**, 147 (1969).

[50] T. H. Dunning, J. Chem. Phys. **53**, 2823 (1970).

[51] T. H. Dunning, J. Chem. Phys. **55**, 716 (1971).

[52] O. Sueoka and S. Mori, J. Phys. B **19**, 4035 (1986).